

Title

Soft tissue abnormalities in Wassel type VI radial polydactyly: a detailed anatomical study

Susumu Saito, MD, PhD¹; Itaru Tsuge, MD, PhD¹; Hiroki Yamanaka, MD, PhD¹; Naoki Morimoto, MD, PhD¹.

Department of Plastic and Reconstructive Surgery, Graduate School of Medicine and Faculty of Medicine, Kyoto University, Kyoto, Japan.

Corresponding author

Susumu Saito

Yoshida-Konoe-cho, Sakyo-ku

Kyoto 606-8501, Japan

Telephone number: +81-75-751-3613

Fax number: +81-75-751-4340

E-mail address: susumus@kuhp.kyoto-u.ac.jp

Keywords

deformity; radial polydactyly; thenar muscles; thumb duplication; ultrasound

Abstract

Wassel VI radial polydactyly is associated with metacarpal adduction and radial deviation of the metacarpophalangeal joint of the ulnar duplicate. The soft tissue abnormalities responsible for these deformities were characterised using preoperative multi-planar three-dimensional ultrasound and intraoperative observation in four patients. In all patients, the abductor pollicis brevis and superficial head of the flexor pollicis brevis inserted into the radial first metacarpal, whereas the adductor pollicis and deep head of the flexor pollicis brevis inserted into the ulnar thumb. Aberrant location of the flexor pollicis longus and absence of the A1 pulley system was associated with severe radial deviation. An additional superficial thenar muscle along the ulnar metacarpal was associated with minimal metacarpal adduction. Uneven forces on the ulnar duplicate could be associated with these characteristic deformities and joint instability. Knowledge of these abnormalities allows better planning of surgery and further insight into this rare radial polydactyly configuration.

Level of evidence: II

INTRODUCTION

Wassel VI radial polydactyly is relatively uncommon, characterized by complete duplication of the first metacarpal and accounting for 3–5% of all radial polydactyly phenotypes (Ogino et al., 1996; Zuidam et al., 2008). These radial polydactyly cases are commonly associated with a narrowed first web and ulnar instability of the metacarpophalangeal (MCP) joint of the ulnar duplicate (Bessho et al., 2020; Ogino et al., 1996). A combination of an abducted radial thumb and an adducted ulnar thumb results in a divergent appearance of the thumb duplications. There are variations in the severity of MCP joint instability, ranging from slight deviation to radial-palmar subluxation of the proximal phalanx. Persistent adduction contractures and MCP joint instability is associated with poor long-term outcome after thumb reconstruction (Makino et al., 2003; Watari et al., 2003). Currently, there is no established surgical method to address these issues.

It is well established that joint instability or deformation has a biomechanical basis; for example, the zigzag deformity in Wassel type IV radial polydactyly can be caused by abnormal positioning of the flexor pollicis longus (FPL) tendon (Marks and Bayne, 1978). Moreover, successful joint stabilisation after FPL tendon realignment suggests that joint instability during early infancy is reversible and imbalanced forces are an important but correctable cause of joint instability (Lee et al., 2013). In Wassel type VI radial polydactyly, findings such as a narrowed first web and MCP joint instability in the ulnar duplicate, features commonly found in thumb hypoplasia, suggest that thenar muscle abnormalities may also be involved. Other possibilities are anomalous insertions of the abductor pollicis longus or adductor muscles. To date, a complete understanding of soft tissue abnormalities in this configuration of radial polydactyly remains lacking.

Recently, a three-dimensional ultrasound technique has been shown to be useful for observing thenar dysplasia in radial polydactyly (Saito et al., 2018). The purpose of this study is to characterise the soft tissue abnormalities associated with adduction of the ulnar metacarpal and radial deviation of the ulnar MCP joint in Wassel type VI radial polydactyly in detail using three-dimensional ultrasound visualisation and direct intraoperative observation.

METHODS

Patients

This prospective study commenced in 2014, after approval was obtained by the ethics committee of our institution. The study was conducted in accordance with guidelines

from the Declaration of Helsinki, including written informed consent for surgery and study participation obtained from a parent of each patient. As there are different subtypes of type VI radial polydactyly, this study was limited to those in which the ulnar thumb is well formed, despite MCP joint instability and angulation. However, the subtype in which there is a well-formed distal part of the ulnar thumb but poorly formed proximal part was excluded, because the proximal MCP joint hypoplasia may complicate analysis of factors influencing joint stability.

Analysis of anatomical structures

The developmental and morphological features of the duplicated thumbs were evaluated using preoperative plain radiographs. The development of the ulnar thumb was evaluated based on the ratio of the ulnar thumb metacarpal (u1MC) length of the affected side to the unaffected side. The development of the radial thumb was evaluated based on the ratio of the radial thumb metacarpal (r1MC) length to u1MC length. Four parameters were used to characterise skeletal morphology: (1) r1MC abduction, measured by the angle between the third metacarpal and r1MC; (2) u1MC adduction, measured by the angle between the third metacarpal and u1MC; (3) divergence, measured by the angle between r1MC and u1MC, and finally (4) MCP joint radial deviation of the ulnar duplicate. MCP joint radial deviation (in the ulnar duplicate) were classified according to four grades: grade 0, instability only; grade 1, $<30^\circ$; grade 2, $30^\circ\text{--}60^\circ$; and grade 3, $\geq 60^\circ$.

The three-dimensional ultrasound scanning method had previously been described (Saito et al., 2016) (Supplemental Video S1). In short, the thenar region was scanned using a linear array transducer (Preirus; Hitachi Aloka Medical, Tokyo, Japan) in a transverse direction at a precisely controlled speed of 3 mm/second. Consecutive images were acquired at 0.2mm intervals and processed to reconstruct three-dimensional data using imaging software (ImageJ; National Institutes of Health, Bethesda, MD, USA). Anatomical identification of structures was accomplished based on multiplanar observations initially using coronal sections, followed by sagittal and axial sections. Especially for coronal sections, images of skeletal outlines were saved and shown in more superficial sections as anatomical references. In addition, planes perpendicular to each metacarpal were used for detailed muscle discrimination. The anatomical findings obtained with ultrasound imaging were combined with observations made intraoperatively.

Muscular nomenclature

Challenges exist in the nomenclature of thenar muscles, due to their anomalous arrangement. In normal anatomy, the flexor pollicis brevis has a superficial head and

deep head (Day and Napier, 1961) and the abductor pollicis brevis and superficial head of the flexor pollicis brevis are located in layers superficial to the FPL, whereas the deep head of flexor pollicis brevis and adductor pollicis are located in layers deep to the FPL. To ensure uniformity, we identified the FPL in the thenar region and used it as a landmark to define superficial components of the thenar muscles. Among the superficial components, musculature that originated at the tubercle of the trapezium or the radial part of the flexor retinaculum were defined as the abductor pollicis brevis, whereas musculature that originated more distally were defined as the superficial head of the flexor pollicis brevis (Van Sint Jan and Rooze, 1992). In the deep components, musculature that had a broad origin around the third metacarpal was defined as the transverse head of the adductor pollicis, and musculature distributed between the adductor pollicis and u1MC was defined as the deep head of flexor pollicis brevis. The oblique head of the adductor pollicis was not defined in this study because it was very difficult to differentiate it from the neighbouring deep head of flexor pollicis brevis (Dunlap et al., 2017). Likewise, the opponens pollicis was not defined because direct observation would require unnecessary dissection by peeling off the overlying abductor pollicis brevis and superficial head of the flexor pollicis brevis (Van Sint Jan and Rooze, 1992). Location of each thenar muscle was recorded using a section and level classification system for the carpal and metacarpal region (Figure 1). For muscle origin, 12 regions were defined based on the location of the tubercle of the trapezium and carpal tunnel. For muscle insertion, five levels were defined along the metacarpal of each thumb.

RESULTS

Patients

Four consecutive patients, all male, with complete Wassel VI metacarpal duplication were included into this study from 2014 (Table 1). The right hand was affected in all cases, and the mean ages at the time of the ultrasound examination and surgery were 15 months (range, 6 to 30 months) and 19 months (range, 14 to 30 months), respectively.

When comparing the u1MC lengths between the affected hand and the normal hand, the mean ratio was 1.0 (range, 1.0 to 1.1). When comparing the radial thumb metacarpal (r1MC) length to u1MC length, the mean ratio was 0.75 (range, 0.6 to 0.8). These results confirmed our initial observations that the ulnar duplicate was the dominant of the two, and its morphology was 'near normal' in terms of size whereas the radial duplicate was more hypoplastic. Morphological characteristics of the four patients, including their respective skeletal features and arrangements of extrinsic and intrinsic

muscles are as detailed in Figure 2. Every patient had r1MC abduction of at least 90° or more.

Degree of divergence of the two duplicates

Patient 1 was characterised by minimal u1MC adduction with mild intermetacarpal divergence (Figures 2 and 3). Patient 2 was characterised by u1MC adduction of around 30° and intermetacarpal divergence of around 70°. Patients 3 and 4 had both marked intermetacarpal divergence exceeding 90° and less than 15° of u1MC adduction.

Degrees of MCP joint deviation and associated anatomy

Grade 3 MCP joint radial deviation in the ulnar duplicate was observed in Patient 3 (Figure 4), whereas the others had grade 1 MCP joint radial deviation. In all four patients, the abductor pollicis brevis arose at the tubercle of the trapezium or the surface of the flexor retinaculum in the radial row of the carpal tunnel and inserted into the middle (Patients 2 and 3) or proximal (Patients 1 and 4) diaphysis region of the r1MC. Distribution of the superficial head of flexor pollicis brevis was similar; it arose at the surface of the distal flexor retinaculum in the radial row of the carpal tunnel and had a conjoined insertion with the abductor pollicis brevis. Notably, an additional superficial muscle was observed along the u1MC in Patient 1 (Figure 5). Both the adductor pollicis and deep head of flexor pollicis brevis were ulnar to the u1MC in all cases.

The FPL was ulnar to the u1MC in Patients 1, 2, and 4. However, in Patient 3, it traversed the u1MC and ran on the radial side of the u1MC toward the base of the deviated proximal phalanx. Direct observation confirmed the absence of the normal A1 pulley system along the FPL. Instead, there was a flat, aponeurotic connection in the intermetacarpal space suggestive of an A1 remnant (Figure 6), which was not observed in the other patients.

Surgical correction

Surgical procedures performed included resection of the radial duplicate, first web widening using Z-plasties, preservation of the ulnar FPL tendon and extensor tendons, and reattachment of the abductor pollicis longus, abductor pollicis brevis and superficial head of the flexor pollicis brevis to the ulnar duplicate. No osteotomy was performed. In all patients, the detached abductor pollicis brevis and superficial head of the flexor pollicis brevis were not long enough to reach beyond the ulnar MCP joint. They were reinserted into the dorsal aponeurosis of the extensor system proximal to the MCP joint.

DISCUSSION

In this study, soft tissue abnormalities as evident from detailed imaging techniques and intraoperative findings revealed several consistencies of muscle attachments, such as

insertion of the abductor pollicis brevis and superficial head of the flexor pollicis brevis into the radial first metacarpal, whereas the adductor pollicis and deep head of flexor pollicis brevis inserted into the ulnar thumb. We also found an aberrantly located FPL and absence of the normal A1 pulley system in one patient with severe radial deviation of the MCP joint.

Although adduction deformity of the ulnar duplicate in type VI radial polydactyly has been described in the literature (Bessho et al., 2020; Ogino et al., 1996), its anatomical basis has not been well discussed. In normal thumb anatomy, muscles associated with first metacarpal abduction include the abductor pollicis longus tendon, abductor pollicis brevis, and opponens pollicis (McFarlane, 1962). In type VI radial polydactyly, the abductor pollicis longus tendon always attaches to the base of the r1MC and not to the u1MC. In addition, we observed aberrant insertions of the abductor pollicis brevis and superficial head of flexor pollicis brevis into the proximal to middle portion of the r1MC. Theoretically, these abnormalities might change the balance of kinematic conditions around the u1MC, making it prone to an adduction deformity. In Patient 1, there was an additional superficial muscle along the u1MC, which might function as an abductor and to minimize the adduction deformity.

Likewise, the anatomical and biomechanical aspects underlying the cause of radial deviation of the MCP joint in the ulnar duplicate has not been well studied. Characteristic morphological and soft tissue abnormalities were found in Patient 3 who had two divergent metacarpals and two convergent proximal phalanges. The location of the FPL was shifted to the radial side of the u1MC with an aponeurotic extension, which might be the remnant of an A1 pulley. These findings were very similar to the morphological and soft tissue features in type IV radial polydactyly with a zigzag deformity. In this subtype, the location of the FPL on the radial side of the proximal phalanx and absence of the A2 pulley may have contributed to the MCP joint divergence and interphalangeal joint convergence (He and Nan, 2016; Lee et al., 2013).

In normal anatomy, the abductor pollicis brevis and adductor pollicis have symmetrical distal attachments to the sesamoid bones on the volar side and the extensor system on the dorsal side, which comprise a dynamic stabilisation system around the MCP joint (McFarlane, 1962). The radial sesamoid also has attachments to the superficial and deep head of flexor pollicis brevis, with some variations (Day and Napier, 1961). In Patients 1, 2, and 4, there was grade 1 MCP joint radial deviation in the ulnar duplicate despite a normal location of the FPL. In these patients, dysfunction of the dorsal ulnar dynamic stabilizers and uneven flexion forces on the MCPJ joint from the deep head of flexor pollicis brevis might be associated with MCP joint

instability and deviation (Figure 7a). From a biomechanical perspective, forces acting on the radial side of the proximal phalanx in Patient 3 might be a cause of MCP joint radial deviation and carpometacarpal joint adduction in the ulnar duplicate (Figure 7b).

Understanding which patients might develop progressive radial deviation after reconstruction is in the surgeon's interest. Watari et al. (2003) reported that nine of 20 patients with metacarpal duplication had adduction deformity and abductor pollicis brevis weakness at 3 years after surgery. Makino et al. (2003) reported long-term follow-up of patients with type V and type VI radial polydactyly, with 60 % of patients required revision surgery but 80% of these patients who underwent revision surgery did not have any functional improvement. Bessho et al. (2020) reported short-term surgical outcomes of 12 patients with type VI radial polydactyly; three of the five patients with MCP joint radial deviation and one out of seven patients without MCP joint radial deviation required revision surgery, including opponensplasty with stabilisation on the ulnar side of the MCP joint or reuse of the transferred abductor pollicis brevis for joint stabilisation. In our patients, the abductor pollicis brevis and superficial head of the flexor pollicis brevis were not long enough to reach the MCP joint. It is unclear whether that the transferred hypoplastic abductor pollicis brevis and superficial head of the flexor pollicis brevis can improve the degree of ulnar deviation.

Our study has several limitations. The sample size was small, as this was a relatively uncommon condition. In addition, we only wanted to include patients in which the ulnar thumb was within the normal range of development, so as to minimise the possible influence of ulnar thumb hypoplasia on radial MCP joint instability (Watari, 1981). We also did not report functional outcomes after surgery, as we did not think it was the focus of this study.

In conclusion, this study characterised soft tissue abnormalities in type VI radial polydactyly. Positional abnormalities of the thenar muscles and FPL and uneven forces acting on the MCP joint could be associated with deformities and joint instability found in type VI radial polydactyly. Understanding the anatomical abnormalities in type VI radial polydactyly may be useful in predicting prognosis after surgery and may contribute to developing new surgical strategies.

References

Bessho Y, Takagi T, Seki A, Takayama S. Treatment for Wassel types V and VI thumb polydactyly. *J Hand Surg Asian Pac.* 2020, 25: 153-7.

Day MH and Napier JR. The two heads of flexor pollicis brevis. *J Anat.* 1961, 95:123-30.

Dunlap SS, Aziz MA, Ziermann JM. Anatomical variations of the deep head of Cruveilhier of the flexor pollicis brevis and its significance for the evolution of the precision grip. *PLoS One.* 2017, 9;12:e0187402.

He B, Nan G. Causes of secondary deformity after surgery to correct Wassel type IV-D thumb duplication. *J Hand Surg Eur.* 2016, 41: 739-44.

Lee CC, Park HY, Yoon JO, Lee KW. Correction of Wassel type IV thumb duplication with zigzag deformity: Results of a new method of flexor pollicis longus tendon relocation. *J Hand Surg Eur.* 2013, 38: 272-80.

Makino H, Horii E, Nakamura R. Long-term follow-up of surgical outcome for thumb polydactyly. *J Jpn Soc Surg Hand.* 2003, 20: 185-8.

Marks TW, Bayne LG. Polydactyly of the thumb: Abnormal anatomy and treatment. *J Hand Surg Am.* 1978, 3:107-16.

McFarlane RM. Observations on the functional anatomy of the intrinsic muscles of the thumb. *J Bone Joint Surg.* 1962, 44: 1073-88.

Ogino T, Ishii S, Takahata S, Kato H. Long-term results of surgical treatment of thumb polydactyly. *J Hand Surg Am.* 1996, 21: 478-86.

Saito S, Ueda M, Murata M, Suzuki S. Thenar dysplasia in radial polydactyly depends on the level of bifurcation. *Plast Reconstr Surg.* 2018, 141: 85e-90e.

Saito S, Ueda M, Takahashi N, Kawakatsu M, Suzuki S. Three-dimensional ultrasonography for visualization of muscular anomalies in type VI and VII radial polydactyly. *Skeletal Radiol.* 2016, 45: 541-7.

Van Sint Jan S, Rooze M. The thenar muscles. New findings. *Surg Radiol Anat.* 1992, 14: 325-9.

Watari S, Nakamura M, Masumoto A. Thumb polydactyly: Results of long-term follow-up after surgery. *J Jpn Soc Surg Hand.* 2003, 20: 509-15.

Watari S. Anomalies of the hand. In: Sato K, Tsuge K (Eds). *Shin Rinsho Seikeigeka Zensho* Kanahara Publishing Co., LTD.,1981, Vol. 8A: 158-65.

Zuidam JM, Selles RW, Ananta M, Runia J, Hovius SE. A classification system of radial polydactyly: Inclusion of triphalangeal thumb and triplication. *J Hand Surg Am.* 2008, 33: 373-7.

Table 1. Summary of skeletal characteristics and soft tissue abnormalities of type VI radial polydactyly patients included in this study

Patient	Age at exam. (mth)	Affected side	u1MC adduction (degree)	MCPJ radial deviation†	Insertion of AbPB and FPBs	Insertion of AdP and FPBd	Additional muscles for abduction	Aberrant FPL and A1 pulley
1	14	R	45	grade 1	r1MC	u1MC	+	-
2	30	R	33	grade 1	r1MC	u1MC	-	-
3	9	R	2	grade 3	r1MC	u1MC	-	+
4	6	R	14	grade 1	r1MC	u1MC	-	-

AbPB: abductor pollicis brevis; AdP: adductor pollicis; FPBs and FPBd: superficial and deep heads of the flexor pollicis brevis, respectively; FPL: flexor pollicis longus. MCPJ: metacarpophalangeal joint; r1MC and u1MC: first metacarpal of the radial and ulnar thumbs, respectively. †: grade 1, <30°; grade 2, 30°–60°; and grade 3, ≥60°

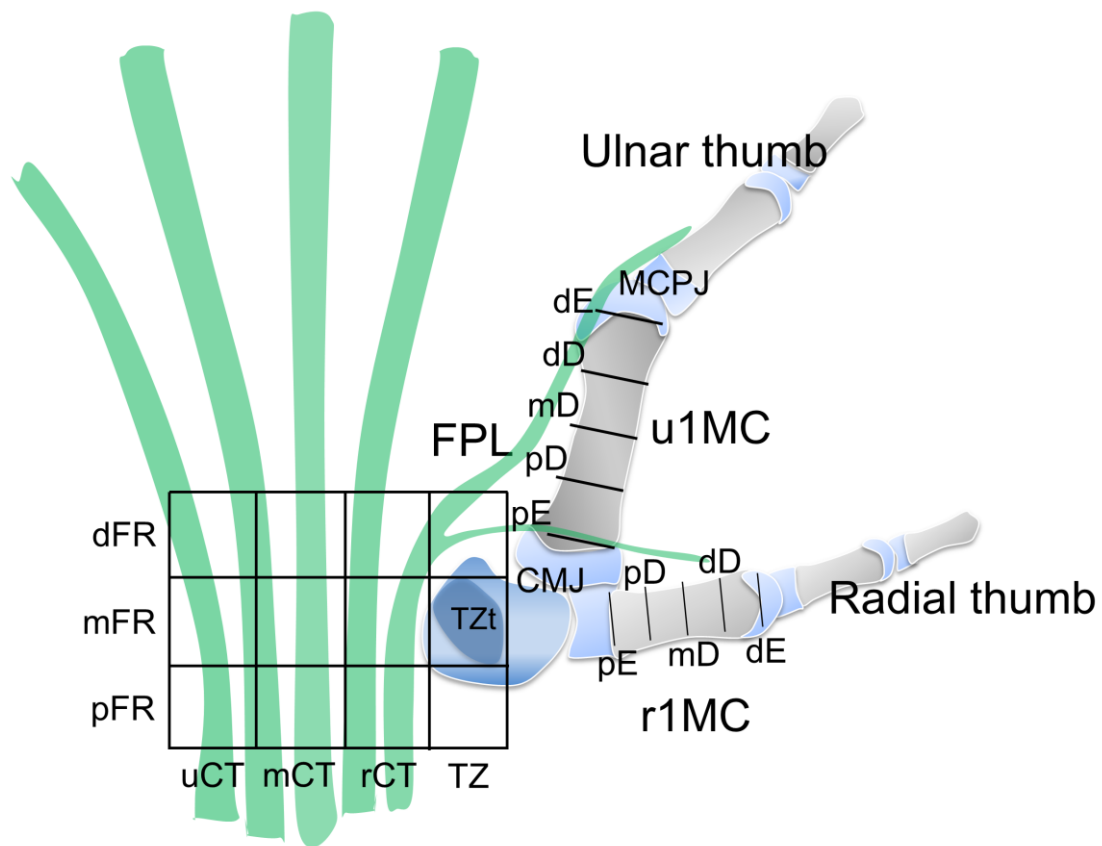


Figure 1. Region and level classification system.

Twelve sections were defined for the carpal region based on the location of the tubercle of the trapezium (TZ) and carpal tunnel (CT). Five levels were defined along each metacarpal. Lower case letters d, m, p, r, and u indicate distal, middle, proximal, radial, and ulnar, respectively.

CMJ: carpometacarpal joint; D: diaphysis; E: epiphysis; FPL: flexor pollicis longus; FR: flexor retinaculum; MCPJ: metacarpophalangeal joint; r1MC and u1MC: first metacarpal of the radial and ulnar thumbs, respectively; TZt: tubercle of the TZ.

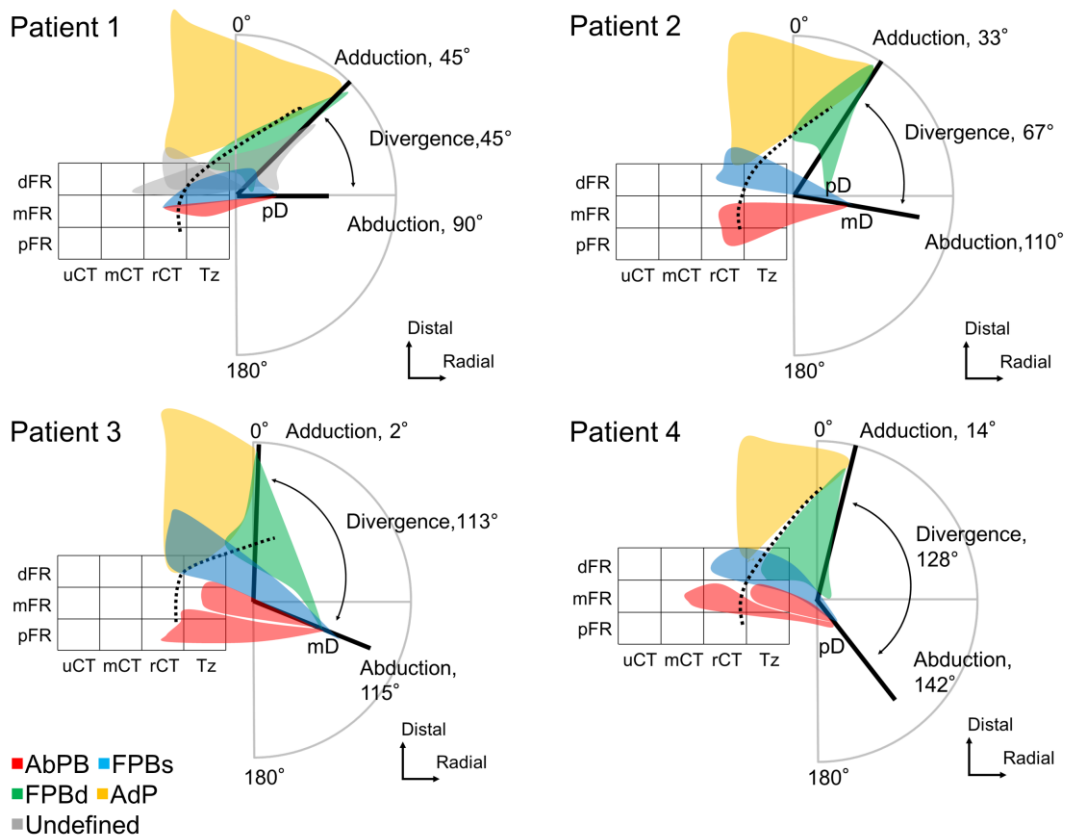


Figure 2. Schematic representation of skeletal features and locations of the thenar muscles and flexor pollicis longus in patients with type VI.

The black lines represent the duplicated metacarpals and their morphology. The length of the line on the radial side reflects the developmental index of the radial metacarpal. The coloured figures represent the thenar muscles. The dotted lines indicate the location of the flexor pollicis longus. Lower case letters d, m, p, r, and u indicate distal, middle, proximal, radial, and ulnar, respectively.

AbPB: abductor pollicis brevis; AdP: adductor pollicis; CT: carpal tunnel; D: diaphysis; FPBs and FPBd: superficial and deep heads of the flexor pollicis brevis, respectively; FR: flexor retinaculum; TZ: trapezium.



Figure 3. Preoperative radiograph (oblique view) of Patient 1 shows grade 1 ($<30^\circ$) radial deviation of the metacarpophalangeal joint of the ulnar thumb.



Figure 4. Preoperative radiograph (oblique view) of Patient 3 shows grade 3 ($\geq 60^\circ$) radial deviation of the metacarpophalangeal joint of the ulnar thumb.

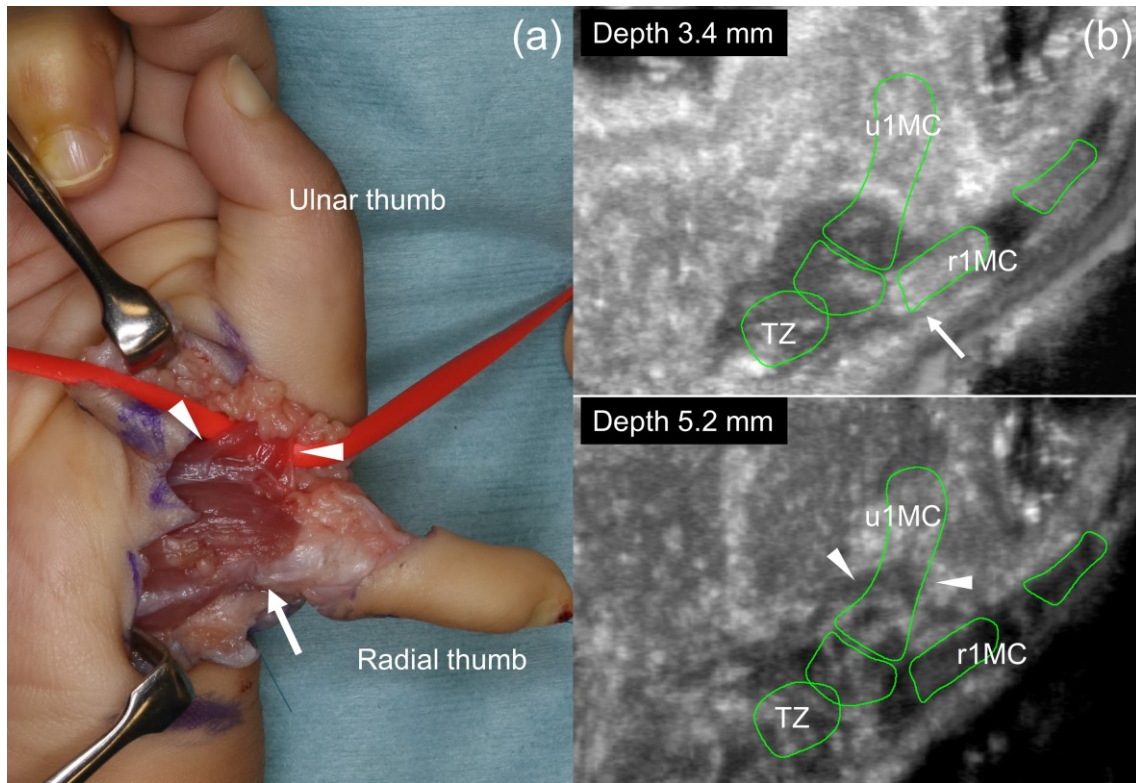


Figure 5. Intraoperative photograph (a) and coronal ultrasound images at different depths (b) from Patient 1 show the conjoined insertion of the abductor pollicis brevis and superficial head of the flexor pollicis brevis to the radial first metacarpal (arrows) and the presence of an additional thin, flat muscle in the radial aspect of the u1MC (arrowheads). Green lines indicate skeletal outlines. r1MC and u1MC: first metacarpal of the radial and ulnar thumbs, respectively. TZ: trapezium.

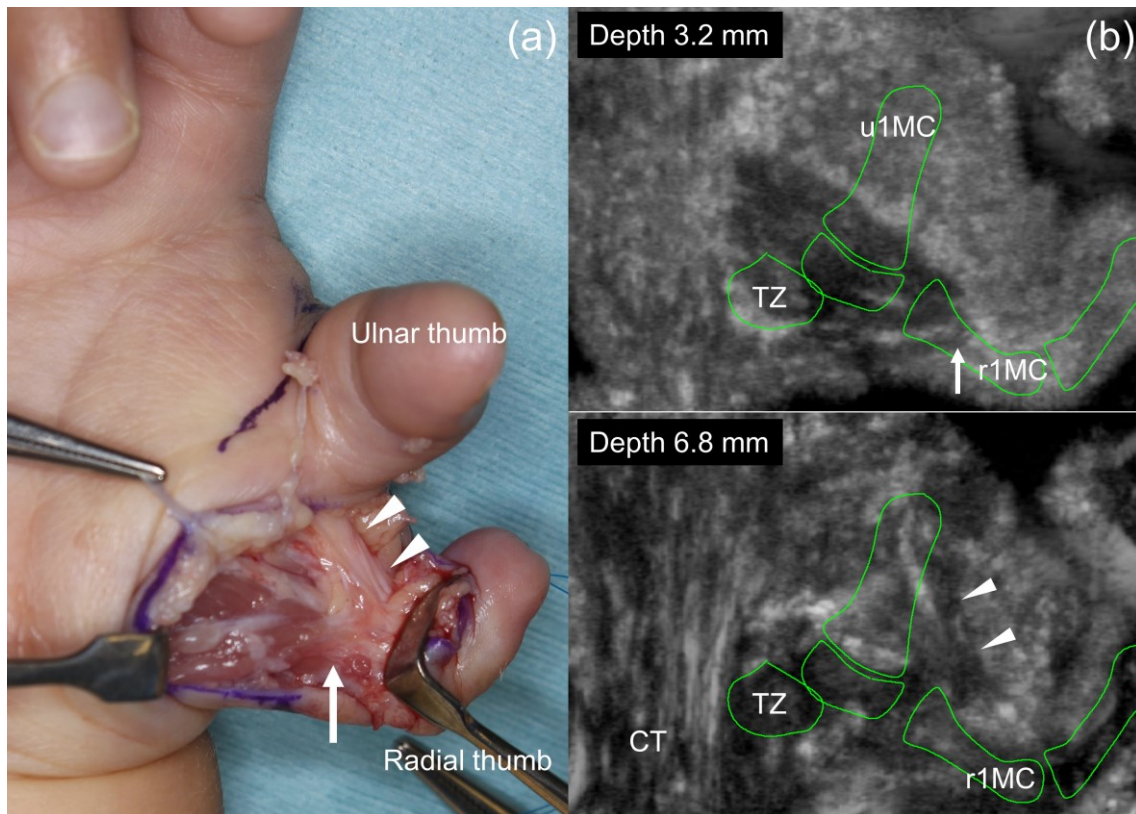


Figure 6. Intraoperative photograph (a) and coronal ultrasound images at different depths (b) from Patient 3 show the conjoined insertion of the abductor pollicis brevis and superficial head of the flexor pollicis brevis to the radial first metacarpal (arrows) and the presence of aponeurotic tissue connecting the heads of the radial and ulnar metacarpals (arrowheads). Note that two deviated proximal phalanges made a convergent appearance, like the convergent distal phalanges in type IV with the zigzag deformity. Green lines indicate skeletal outlines. CT: carpal tunnel; r1MC and u1MC: first metacarpal of the radial and ulnar thumbs, respectively; TZ: trapezium.

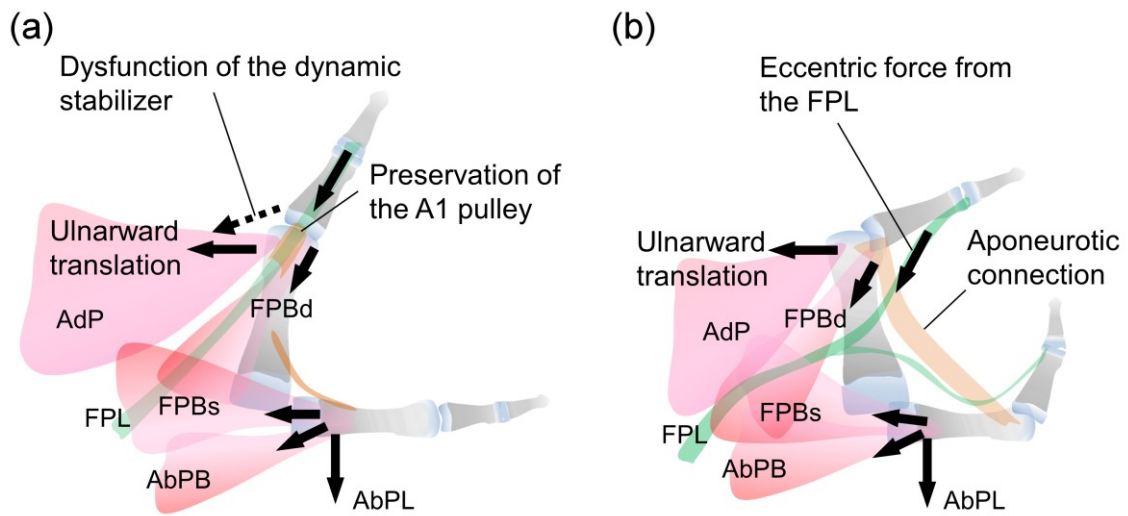
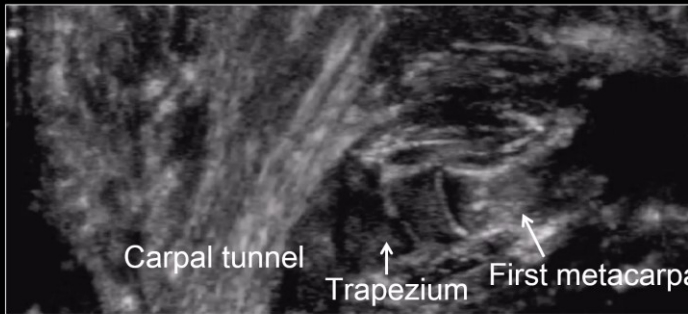
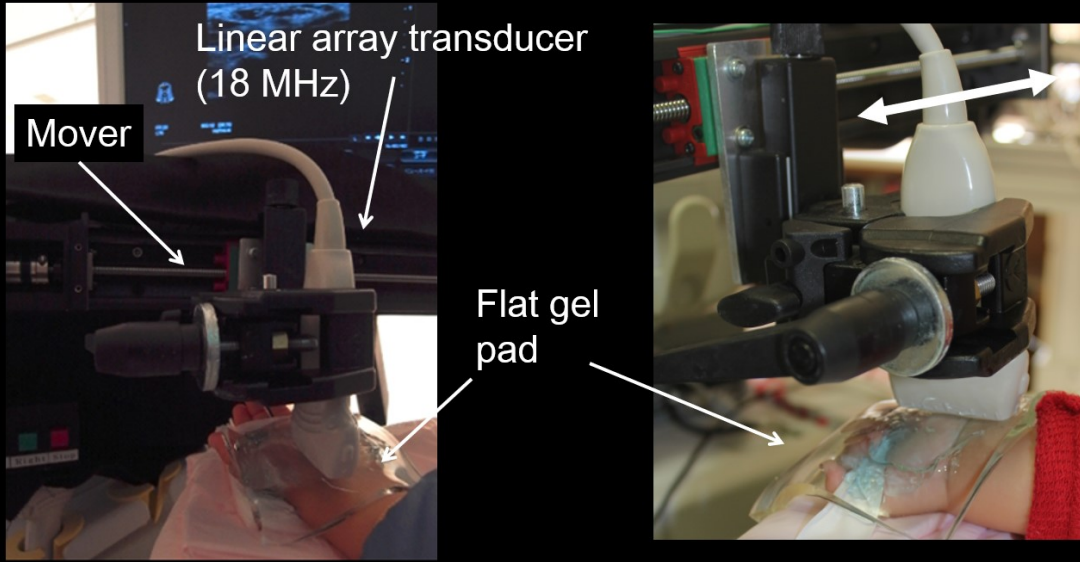


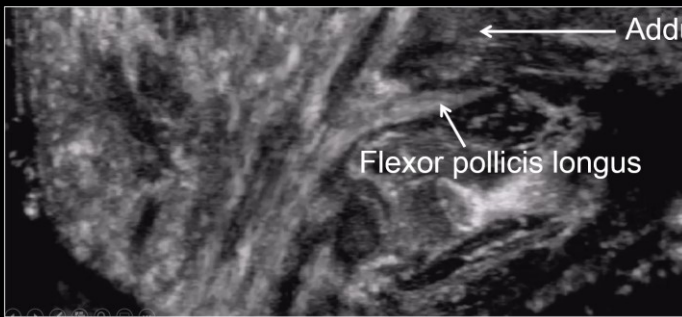
Figure 7. Schematic illustrations showing soft tissue abnormalities and associated mechanisms for metacarpal adduction and radial metacarpophalangeal joint instability (a) and convergent deformity of the proximal phalanges (b). AbPB: abductor pollicis brevis; AbPL: abductor pollicis longus; AdP: adductor pollicis; FPBs and FPBd: superficial and deep heads of the flexor pollicis brevis, respectively; FPL: flexor pollicis longus.

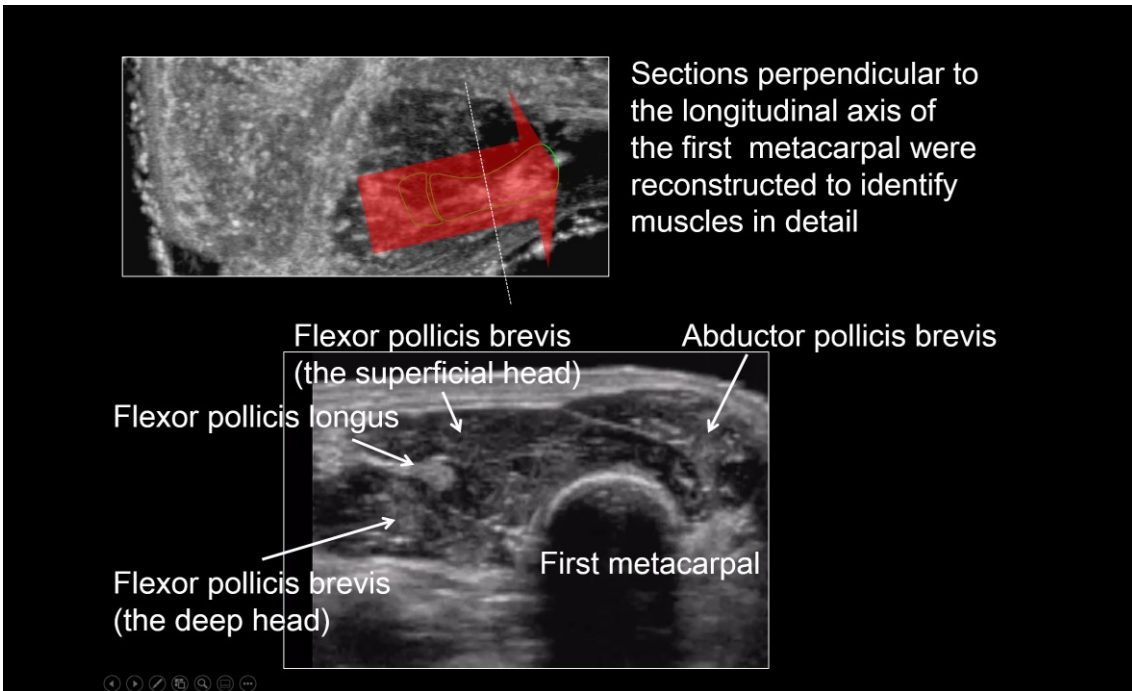
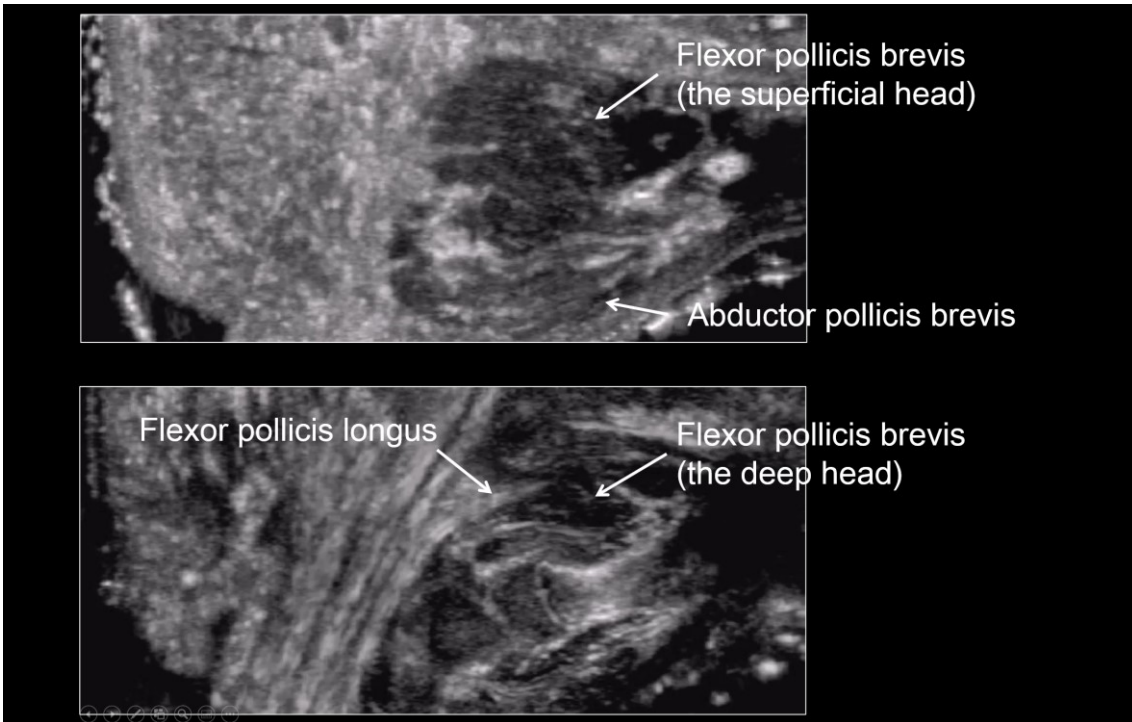
Traditional 3D ultrasound method

An electronic-controlled mover was used to regulate the scanning speed at 3 mm/s



Coronal images were reconstructed to observe horizontal distributions of the thenar muscles





Supplemental Video S1. Video showing the three-dimensional ultrasound examination process and basic methods for anatomical identification